International Journal of Engineering, Science and Mathematics
Vol.6Issue 6, October2017,
ISSN: 2320-0294 Impact Factor: 6.765
Journal Homepage: http://www.ijesm.co.in, Email: ijesmj@gmail.com Double-Blind Peer Reviewed Refereed Open Access International Journal - Included in the International Serial Directories Indexed & Listed at: Ulrich's Periodicals Directory ©, U.S.A., Open J-Gage as well as in Cabell's Directories of Publishing Opportunities, U.S.A

DSP Based Rician Noise Removal in MR Images Using Gradient Projection Algorithm

D. Nedumaran*
J. Papitha**

Abstract

Rician noise in Magnetic Resonance images affects the image contrast, signal dependent bias and signal to noise ratio value. The combined Gabor filter with Gradient projection filter was developed to remove the Rician noise in Magnetic Resonance images and compared its performance with the state-of-the-art filtering methods. The algorithm was developed in the TMS320C6713DSK, which exhibited improvements in the image quality and signal to noise ratio value. Further, it reduces the noise component and preserves the image features with less execution time. For testing the noise removal algorithm, two different levels of Rician noise were added with the raw MR images and removed using the popular and the proposed method. The performance of the proposed method was compared with the popular methods through the estimation of quantitative metrics and visual inspection.

Keywords:

Gradient projection;
DSP;
Rician noise;
Gabor filter;
MRI;
Real time implementation;
PSNR.

Author correspondence:

D. Nedumaran,
Central Instrumentation & Service Laboratory, University of Madras, Guindy Campus, Chennai 600 025, TN, India.

1. Introduction to Rician noise in MR Image

In magnetic resonance (MR) imaging, the array of complex-valued MR data is converted into magnitude image through amplitude estimation during image reconstruction [1] and the reconstructed MR images have artifacts due to pulse timing error, eddy current, phase shift and change in coil impedance in real and imaginary channels. The artifacts affect one of the parameters of the magnitude image data such as field strength, field of view, matrix size, slice thickness, number of excitation and bandwidth, which in turn degrades the quality of the MR image and suffers from low signal to noise ratio (SNR). As a result, there is a bias in noise distribution that reduces the contrast between bright and dark areas. The noise in the magnitude image is assumed to be Rician distribution, since the noise added into both the real and imaginary parts of the image causes random fluctuations. This leads to a signal dependent bias in the data of low-signal regions [2, 3]. Isolating the noise from the signal is a tedious process and many researchers have been attempted this problem and some of the related literature are presented below.

Mohan et al. analyzed different types of denoising methods using transform and statistical based filters and compared their performance in removing the Rician noise [4]. Coupe et al. proposed a robust Median Absolute Deviation (RMAD) estimator in the wavelet domain for removing the Rician noise on the real and synthetic images [5]. Misra et al. proposed the combination of crossover and adaptive mutation of genetic operator for enhancing the convergence rate and quality of GA for effective removal of Rician noise in MR images [6-8]. An edge-preserving Contourlet transform was developed for denoising the PET, MRI-PET and PET-CT images corrupted with Rician noise [9]. Daessle et al. studied the performance of the improved Non Local Means (NLMeans) filter for Rician noise removal in low-SNR and diffusion-weighted MR images [2, 10]. Pizurica et al. analyzed various types of wavelet filters for removing the Rician noise [11,

*&**Central Instrumentation & Service Laboratory, University of Madras, Guindy Campus, Chennai 600 025, TN, India.

12]. Sijbers and co-researchers [13-16] studied thoroughly the intricacies of maximum likelihood approach in removing the Rician noise over the other conventional techniques. Pereza et al. specially designed a new method to estimate the Rician noise level present in MR images by matching the noise-free slices after adding known levels of noise [17].

Rice demonstrated that the Rician PDF as the SNR of the signal and Marzetta applied an expectation-maximization (EM) algorithm to SAR images for estimating the parameters of multivariate complex Rician density [18]. The moments of the Rician PDF is expressed in (1).

$$E[m^{v}] = (2\sigma^2)^{v/2}\Gamma\left(1+\frac{v}{2}\right)_1 F_1\left[-\frac{v}{2};1;-\frac{A^2}{2\sigma^2}\right] \tag{1}$$

where A is the real-phase MR image without noise and σ^2 is the noise variance. The even moments of the Rician distribution (i.e., when v is even) are simple polynomials, whereas the odd moments are more complex [19, 20].

The measured pixel intensity by magnitude signal *M(x)* is the Rician distributed envelope of the complex signal *P(x)* given by (2).

$$M(x) = |P(x)| \tag{2}$$

By expressing $P(x, y; A, \sigma)$ in terms of the polar coordinates $x = M\cos\theta, y = M\sin\theta$ the probability distribution of the magnitude image pixel intensity can be derived. Further, $P(x, y; A, \sigma)$ is multiplied by the Jacobian determinant $\frac{\partial(x,y)}{\partial(M,\theta)} = M$ and then integrating over the angular variable θ results in the Rician distribution given by (3).

$$P(M; A, \sigma) = \frac{M \exp\left\{-(M^2 - A^2)/2\sigma^2\right\} I_o(MA/\sigma^2)}{\sigma^2} \tag{3}$$

where$M$ is the zero-order Bessel function [1].

Several techniques have been reported in the literature to remove the Rician noise, but still there is no perfect filtering method available to remove Rician noise completely without the loss of image information. One such attempt was tried in this work by developing a novel Gabor filter with Gradient projection algorithm for removing Rician noise effectively and for improving the quality of the MR image.

2. Methods

a. Gradient Projection Method

Usually, gradient is used to find the function of many variables through the generalization of the concept of derivation [21]. The gradient of the scalar field is the vector of the partial derivative function. The gradient point direction increases in the magnitude direction and the final magnitude of the gradient is obtained using the Equation 4.

$$|G| = |Gx| + |Gy| \tag{4}$$

The gradient-projection algorithm (GPA) is a powerful method for solving constrained minimization problems and used in conjunction with other methods for achieving faster rate of convergence [22-24]. Bonettini et al. proposed scaled gradient projection method using global convergence properties and the step length parameter that improved the convergence rate for solving image deblurring problems [25-28]. A scheme based on the projected gradient algorithm, which computed the decomposition models for colour images was implemented by Duval et al. [29]. Seo et al. combined the projection method with the constraint least squares (CLS) method for effectively removing the blocking artifacts present in the H.264 video coding standard [30]. Loris et al. implemented the gradient projection algorithm for constrained sparse recovery from noisy data [31]. In 1982, Bertsekas derived some results for a projected Newton Method [32] and Gafini and Bertsekas found the solution for a 2-metric projection method [33]. Becky and Teboulle studied the image denoising, deblurring and signal recovery problems based on the discretized total variation (TV) minimization models using the gradient algorithms [34].

The convex minimization with large scale data set of inverse problems was solved by the proximal-gradient methods.For minimizing the continuously differentiable mapping on non-empty closed convex set C, the constrained minimization problem can be represented as,

$$\min_{x \in C} f(x) \tag{5}$$

where the object function $f(x)$ is a composite type convex function denoted by equation 6

$$f(x) = F(x) + G(x) \tag{6}$$

where *G(x)* is the continuous non-smooth convex function and $F(x)$ is the smooth convex function. To solve the minimization problem given in Equation 5, the GP algorithm was employed, which generates a sequence of $\{x_k\}$ through the recursion process given by the Equation 7.

$$x_{k+1} = P_c(x_k - \alpha_{k+1}\nabla f(x_k)) \tag{7}$$

In Equation 7, the initial guess is chosen arbitrarily as $x^0 \in C$ and α_k as a sequence of step sizes with $\alpha_{k+1} \geq 0$ for each $k \geq 0$ and P_c is the orthogonal projection operator on the set *C*. By applying a special case of backward-forward splitting method, the basic Gradient-based model can be written as,

$$x_{k+1} = \arg\min_x \{G(x) + (1/2\alpha_{k+1})\|x - (x_k - \alpha_{k+1}\nabla f(x_k))\|^2\} \tag{8}$$

The image module is given by (9).

$$x + \lambda = b \tag{9}$$

where *b* is the observed noisy data, *x* is the desired unknown image to be recovered and λ is the regularization parameter with $\lambda > 0$.

The image denoising problem was formulated as a constrained problem given by (10).

$$\min_x \|x - b\|_F^2 + 2\lambda|x|_{TV} \tag{10}$$

where the bounds are imposed to reflect the fact that the entries are light intensity of image pixels, hence their values typically fall within, say, the interval of *0-255*. The basic idea to construct the dual problem is like that of the unconstrained problem of minimizing the objective function without the box constrained, which can be solved by the gradient-based algorithm. To describe the algorithm, we need to define four more parameters.

Let *P* be the set of matrix pairs *(p, q)*, *L* denotes the linear operator that maps an element *(p, q)* and the adjoint of the operator *L* is denoted by *LT*. The orthogonal projection operator on convex set *C* is denoted as P_c.If $(p,q) \in P$, then the optimal solution of the dual problem with TV based denoising is given by (11) and (12).

$$\min_{(p,q)\in P} \{h(p,q) \equiv -\|H_c(b - \lambda \sqcap (p,q)\|_F^2 + \|b - \lambda \sqcap (p,q)\|_F^2\} \tag{11}$$

Here $H_c = x - P_c(x)$ for every x (12)

where P_p is the projection operator which maps a matrix pair (p,q) with another matrix pair $(r,s) = P_p(p,q)$ and can be readily implemented [35]. For the better rate of convergence, the Gradient Projection (GP) method is used on the dual problem stated in (13). Considering $(r_1, s_1) = (p_0, q_0)$ at step 0 and *k* at step *k*, the Equation 7 can be denoted as (13), (14), (15) and (16).

$$(p_{k+1}, q_{k+1}) = P_p[(r_{k+1}, s_{k+1}) + (1/8\lambda) \sqcap^T (P_c[b - \lambda \sqcap (r_{k+1}, s_{k+1})])] \tag{13}$$

$$\alpha_{k+2} = \{1 + \sqrt{1 + 4\alpha_{k+1}^2}\}/2 \tag{14}$$

$$(r_{k+2}, s_{k+2}) = (p_{k+1}, q_{k+1}) + [(\alpha_{k+1} - 1)/\alpha_{k+2}](p_{k+1} - p_k, q_{k+1} - q_k) \tag{15}$$

$$x^* = P_{B_{l,u}}[b - \lambda L(p_{k-1}, q_{k-1})] \tag{16}$$

b. Gabor Filter

Two Dimensional Gabor filter is a Gaussian kernel function modulated by the sinusoidal plane wave and is self-similar.The mathematical expression of two dimensional Gabor filter *g* (*x*, *y*) is denoted by the product of isotropic Gaussian and complex exponential plane wave [36] given in (17).

Complex

$$g(x,y;\lambda,\theta,\psi,\sigma,\gamma) = \frac{\gamma}{2\pi\sigma^2}\exp\left(-\frac{x'^2 + \gamma^2 y'^2}{2\sigma^2}\right)\exp\left(i\left(2\pi\frac{x'}{\lambda} + \psi\right)\right) \tag{17}$$

Real

$$g(x,y;\lambda,\theta,\psi,\sigma,\gamma) = \frac{\gamma}{2\pi\sigma^2}\exp\left(-\frac{x'^2 + \gamma^2 y'^2}{2\sigma^2}\right)\cos\left(2\pi\frac{x'}{\lambda} + \psi\right) \tag{18}$$

Imaginary $$g(x,y;\lambda,\theta,\psi,\sigma,\gamma)=\frac{\gamma}{2\pi\sigma^2}\exp\left(-\frac{x'^2+\gamma^2y'^2}{2\sigma^2}\right)\sin\left(2\pi\frac{x'}{\lambda}+\psi\right) \quad (19)$$

where $$x' = x\cos\theta + y\sin\theta \quad (20)$$

and $$y' = -x\sin\theta + y\cos\theta \quad (21)$$

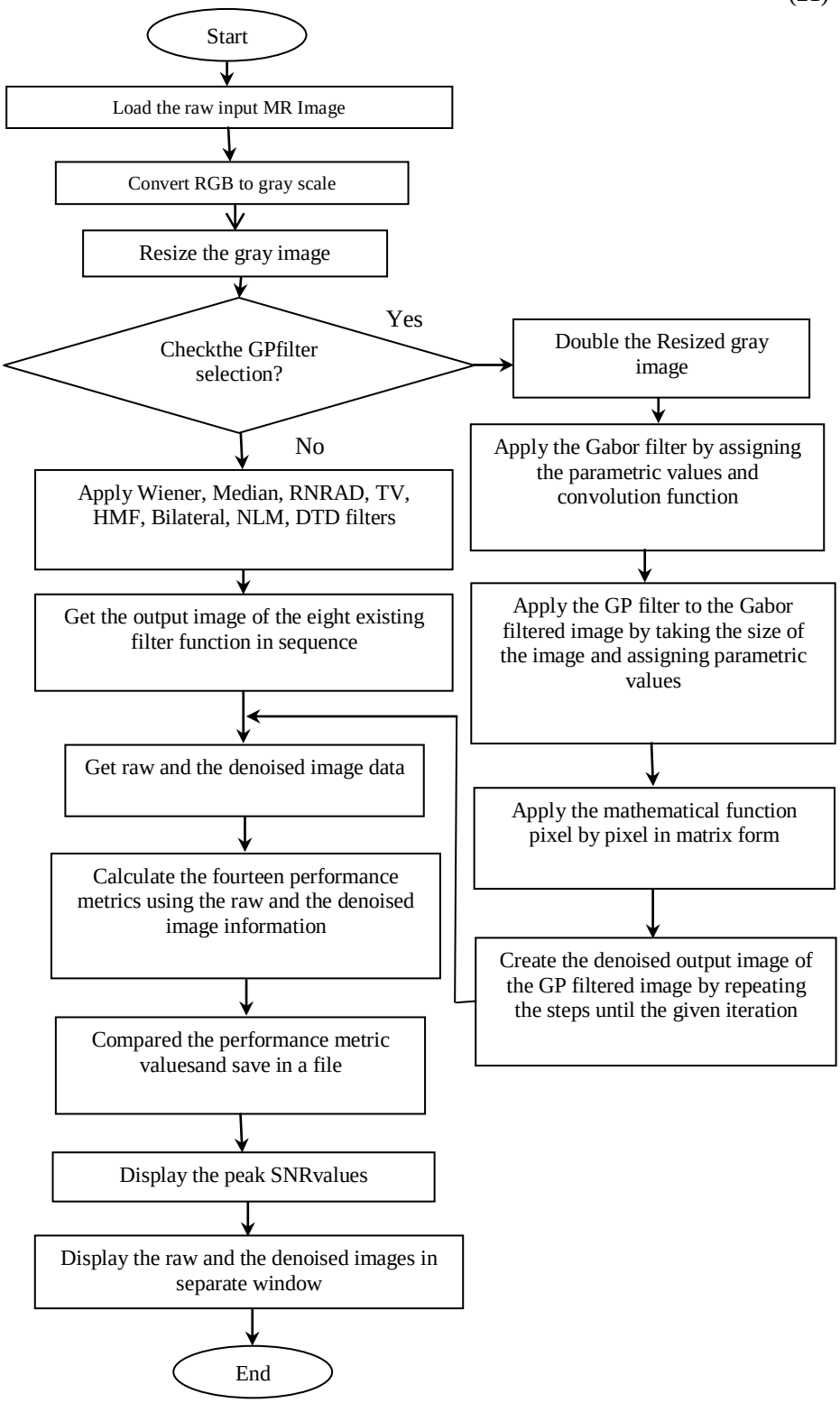

Figure 1: *Flow chart of the proposed GPA+GF algorithm*

In (17), (18) and (19), λ is the wavelengthof the sinusoidal factor, θ is the orientation of the normal to the parallel stripes of a Gabor function, ψ is the phase offset, σ is the standard deviation of the Gaussian envelope and γ represent the spatial aspect ratio that specifies the ellipticity of the Gabor function. The estimated pdfs are used to establish a threshold that minimizes the image-segmentation error. Further, they considered the use of a Gaussian post filter in the analysis. The Gaussian post filter reduces the variance of the Rician-distributed Gabor-filter output, which results in reduced image-segmentation error at the expense of some loss in spatial resolution.

The Gradient Projection Algorithm combined with Gaussian Filter (GPA+GF) algorithm was developed in ANSI C using the code composer studio version 3.1. The flow chart of the developed algorithm is shown in Fig 1. The codes were generated using MATLAB/Simulink 2011b, which are directly ported in the TMS320C6713DSK [37-42], which isinterfaced with the Pentium® Dual-Core CPU E5400 @ 2.70 GHz processor PC operating in Window XP.

3. Results and Analysis

More than 100 MR images were collected and tested with the proposed algorithm. An MR spine image (SP R21.8), added with Rician noise of 0.05 and 0.10 levels was used to demonstrate the proposed GPA+GF filtering performance in removing the Rician noise. A comparative study was attempted with the popular filtering techniques such as Median filter (MF), Wiener filter (WF), Rician noise reducing anisotropic diffusion filter (RNRAD), Total variation filter (TV), Non-local mean (NLM), and Discrete Topological Derivative (DTD). Further, the performance of the filters was studied by estimating the quality metrics from the Rician noise added and their corresponding filtered images. The quality metrics of Peak signal to noise ratio (PSNR) is a measure of ratio between the maximum possible signal power and the noise content. Mean structure similarity index map (MSSIM) is a measure of the similarity between two images by comparing the structure, contrast and the luminance of the image. The contrast to noise ratio (CNR) is the contrast of the image with reference to the background. The image quality index (IQI) measures the degree of distortion in terms of loss of mean distortion, correlation, and variance distortion. The amount of randomness is measured using the metrics Variation of Information (VOI).The raw MR image (SP R21.8), added with Rician noise levels of 0.05 and 0.10 and its corresponding filtered images are shown in Fig. 2 and 3, respectively. The performance metrics estimated for all these images are given in Table 1 for easy comparison.

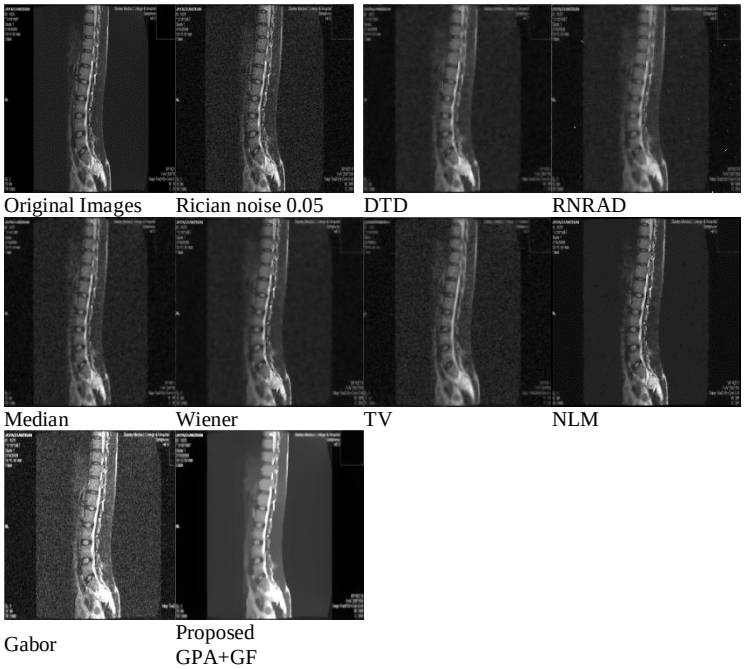

Figure 2:*Original and denoised Spine MR Images (SP R21.8) added with 0.05 Rician noise*

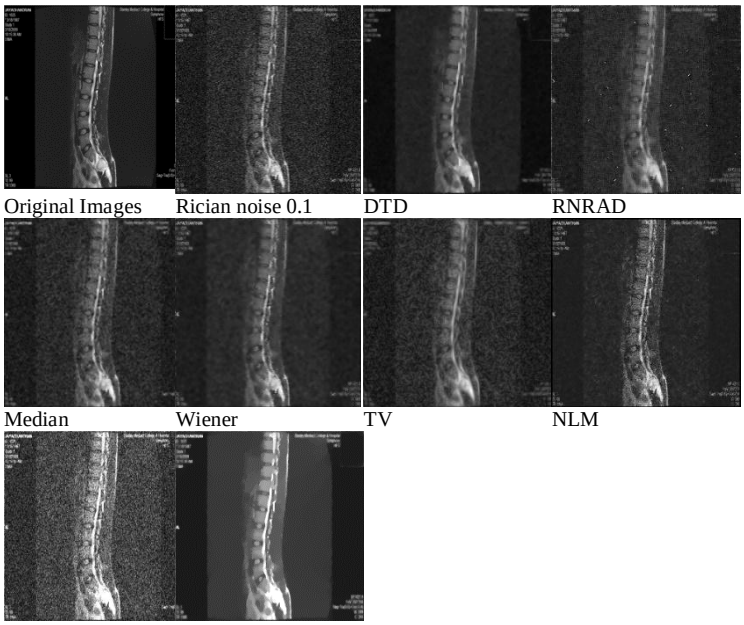

Figure 3. *Original and denoised Spine MR Images (SP R21.8) added with 0.1 Rician noise*

Table 1 Estimated Performance Metrics of the Spine MR Image (SP R21.8) added with 0.05 and 0.1 Rician noise levels

Metrics	**PSNR**		**MSSIM**		**CNR**		**VOI**		**IQI**	
Rician Noise Level	0.5	0.1	0.5	0.1	0.5	0.1	0.5	0.1	0.5	0.1
Median	69.1189	66.142	0.9897	0.9895	0.1257	0.2264	0.117	0.1923	0.8926	0.8133
Wiener	71.368	67.6624	0.9899	0.9916	0.0826	0.1777	0.0702	0.1301	0.9245	0.8494
DTD	62.956	78.2750	0.2447	0.2448	0.0315	0.0315	0.4277	0.4569	0.2045	0.2045
RNRAD	68.9959	66.9607	0.9916	0.9901	0.1029	0.0109	0.129	0.181	0.8838	0.8016
TV	67.6564	65.6249	0.9925	0.9893	0.1967	0.268	0.1434	0.2051	0.8782	0.8052
NLM	75.8034	76.8508	1	0.9846	0.0294	0.0196	0.0297	0.023	0.9067	0.8692
G+GP	83.9911	80.0631	0.9940	0.9939	0.5663	0.5319	0.4287	0.4672	0.9297	0.9009

From the visual inspection of the images by the trained radiologists and the estimated performance metrics, the following inferences are arrived out of this study.

1. The PSNR value of the GPA+GF method was found to be outperformed over the other five standard filters taken for comparison. In some cases, the PSNR values of the DTD filter was found to be slightly higher than the proposed GPA+GF filter with the apparent degradation in IQI. This is due to the smoothing of image details while enhancing the PSNR value. The high PSNR value of the proposed GPA+GF method indicates that the proposed method reduces the Rician noise efficiently while maintaining the image details intact.
2. In this study, the proposed GPA+GF technique exhibited MSSIM values close to unity (unity for optimum similarity) compared to the other filters, which revealed that the proposed method retains the original structure of the image without loss of information.
3. The GPA+GF found to have optimum CNR values, which clearly exhibits its better denoising performance as well as contrast improvement characteristics without loss in image details over other popular methods. This property is useful in viewing the low contrast lesions from the background.
4. The proposed GPA+GF method have high VOI value (closer to unity), which means the proposed method exhibited less variation in image information over the other methods.
5. Upon visual inspection of these images by trained radiologist had the opinion that the proposed GPA+GF algorithm's performance is found to be better in denoising the Rician noise than the other methods. Further, they opined that the proposed method retained the image details better than the other methods with very less information loss compared with the popular methods.

Thus, the proposed GPA+GF filter denoised the Rician noise well over the other method and preserved the edges details without loss of information. This is due to the potential of the Gabor filter that improves the contrast of the image without blurring and efficiency of the Gradient Projection filter that reduces the Rician noise effectively with noticiable improvement in the image quality. The combined effect of these proposed filters yields high contrast enhancement with optimal image quality over the other traditional denoising filters.

In summary, the proposed GPA+GF algorithm outperformed over the other traditional methods taken for comparison, which is evident from the qualitative, quantitative and similarity metrics. Consequently, the GPA+GF method can be recommended as a better choice for denoising the Rician noise in MR image than the other standard denoising filters due to its effective denoising, optimum contrast enhancement, less information loss and better visibility of all regions.

4. Conclusion

In this work, we implemented the combined (GPA+GF) method for removing the different levels of Rician noise present in MRI images in the DSP environment. The performance of the proposed filtering method was estimated quantitatively as well as qualitatively (visual inspection) and compared with the other popular filtering methods. The experimental results showed that the GPA+GF method outperformed in terms of the PSNR, MSSIM, CNR and VOI values, which shows its capability in removing the signal dependent bias, effectively. Additionally, the CNR characteristics of the proposed filter strengthen its usefullness in tissue characterization. Presently, the average execution time of the algorithm was found to be in sec, which can be further refined by using efficient coding, memory management, and other advanced programming concepts.

Ackonwledgment

This work was financially supported by University of Madras through the University Research Fellowship.

References

1. Bernstein M. A., Thomasson D. M., and Perman W. H., "Improved detectability in low signal-to-noise ratio magnetic resonance images by means of a phase-corrected real reconstruction,"*The International Journal of Medical Physics Research and Practice, American Association of Physicists in Medicine*, Vol.16, pp. 813-817, 1989.
2. Daessle N. W., Prima S., Coupe P., Morrissey S. P., and Barillot C., "Rician Noise Removal by Non-Local Means Filtering for Low Signal-to-Noise Ratio MRI, Applications to DT-MRI,"*In: 11th International Conference on Medical Image Computing and Computer-Assisted Intervention. New York, 2008*, Vol. 11, pp. 171-179.
3. Sarode M. V., and Deshmukh P. R., "Performance Evaluation of Rician Noise Reduction Algorithm in Magnetic Resonance Images,"*Journal of Emerging Trends in Computing and Information Sciences*, Vol.2, pp.39-44, 2010.
4. Mohan J., Krishnaveni V., and Guo Y., "A survey on the magnetic resonance image denoising methods,"*Biomedical Signal Processing and Control, Elsevier*, Vol.9, pp. 56–69, 2014.
5. Coupe P., Manjon J. V., Gedamu E., Arnold D., Robles M., and Collins D. L., "An Object-based Method for Rician Noise Estimation in MR Images,"*Medical Image Computing and Computer-Assisted Intervention*, Vol.5762, pp.601-608, 2009.
6. Fan Z., Sun Q., Ji Z., Ruan F., and Zhao L., "A Novel Image Denoising Algorithm based on GA, PDE and TV,"*Proceedings of 2nd International Conference on Next Generation Computer and Information Technology, SERSC*, Vol. 27, pp. 94-98, 2013.
7. Fan Z., Sun Q., Ji Z., Ruan F., and Zhao L., "An Image Filter Arithmetic based on GA, PDE and TV,"*Intl. Jour. of Future Generation Communication and Networking*, Vol.6, pp.147-156, 2013.
8. Misra D., Sarker S., Dhabal S., and Ganguly A., "Effect of using Genetic algorithm to denoise MRI images corrupted with rician noise,"*IEEE International Conference on Emerging Trends in Computing, Communication and Nanotechnology (ICE-CCN)*, 2013, pp. 146-151.
9. Mansoor A., Bagci U., and Mollura D., "Noise adaptive multi-resolution technique to accurately denoise PET",*MRI-PET, and PET-CT images, Journal of Nuclear Medicine*, Vol.55, pp. 2050, 2014.
10. Mathen S. J., and George A., "Analysis of MRI Enhancement Techniques for Contrast Improvement and Denoising,"*International Journal of Current Engineering and Technology*, Vol.4, pp. 3853-3860, 2014.
11. Pizurica A., Wink A. M., Vansteenkiste E., Philips W., and Roerdink J. B. T. M., "A review of wavelet denoising in MRI and ultrasound brain imaging,"*Current Medical Imaging Reviews*, Vol.2, pp. 247-260, 2006.
12. Pizurica A., Philips W., Lemahieu I., and Acheroy M., "A versatile wavelet domain noise filtration technique for medical imaging,"*IEEE Transaction on Medical Imaging*, Vol.22, pp.323–331, 2003.
13. Sijbers J., Dekker A. J. D., Scheunders P., and Dyck D. V., "Maximum-likelihood estimation of Rician distribution parameters,"*IEEE Transaction on Medical Imaging*, Vol.17, pp.357-361, 1998.
14. Sijbers J., Dekker A. J. D., Dyck D. V., and Raman E., "Estimation of signal and noise from Rician distributed data,"*Proceedings of the Intl Con. on Signal Proc. and Com., Spain*, 1998, pp. 140–142.
15. Sijbers J., and Dekker A. J. D., "Maximum likelihood estimation of signal amplitude and noise variance form MR data,"*Journal of Magnetic Resonance Imaging*, Vol. 51, pp. 586–594, 2004.
16. Jiang L. and Yang W., "Adaptive magnetic resonance image denoising using mixture model and wavelet shrinkage,"*Proceedings of VIIth digital image computing: techniques and applications, Sydney, Australia*, 2003.

17. Péreza M. G., Conci A., Moreno A. B., Andaluz V. H., and Hernández J. A., "Estimating the Rician Noise Level in Brain MR Image,"*IEEE Conference on ANDESCON*, 2014.
18. Marzetta T. L., "EM algorithm for estimating the parameters of a multivariate complex Rician density for polarimetric SAR," *IEEE, Conference in Acoustics, Speech, and Signal Processing*, Vol.5, pp. 3651-4, 1995.
19. Landini L., Positano V., and Santarelli M. F., "Advanced Image Processing in Magnetic Resonance Imaging,"*Taylor & Francis Group, LLC*, 2005.
20. Koay C. G., and Basser P. J., "Analytically exact correction scheme for signal extraction from noisy magnitude MR signals,"*Journal of Magnetic Resonance*, Vol.179, pp.317-322, 2006.
21. Ponnaiah G. F. M., Baboo S. S., "Detection of Optic Disc and Hard Exudates using Twin Plane Gradient Windowing Technique,"*Global Journal of Computer Science and Technology: F Graphics & Vision, Global Journals Inc. (USA)*, Vol. 14, 2014.
22. Bertsekas D. P., "Nonlinear programming, Athena Scientific, Belmont,"*Massachusetts*, pp. 22-75 and 223-272, 1995.
23. Goldstein A. A., "Convex programming in Hilbert space,"*Bulletin of the American Mathematical Society*, Vol. 70, pp. 709-710, 1964.
24. Levitin E. S., Polyak B. T., "Constrained minimization problems,"*USSR Computational Mathematics and Mathematical Physics*, Vol.6, pp.1-50, 1966.
25. Bonettini S., Zanella R., and Zanni L., "A Scaled Gradient Projection Method for Constrained Image Deblurring,"*Journal of inverse problem,IOP science*, Vol. 25, pp. 1-23, 2009.
26. Bertero M., Boccacci P., Prato M., and Zanni L.,"Scaled Gradient Projection Methods for Astronomical Imaging,"*New Concepts in Imaging: Optical and Statistical Models, Statistical Models in Signal and Image Processing, EAS Publications Series*, Vol. 59, pp. 325-356, 2013.
27. Porta F., Zanella R., Zanghirati G., and Zanni L., "Limited-memory scaled gradient projection methods for real-time image deconvolution in microscopy,"*Communications in Nonlinear Science and Numerical Simulation, Elsevier*, Vol. 21, pp. 112-127, 2015.
28. Bonettini S., Landi G., Piccolomini E. L., and Zanni L., "Scaling techniques for gradient projection-type methods in astronomical image deblurring,"*International Journal of Computer Mathematics, Taylor & Francis*, Vol. 90, pp. 9-29, 2013.
29. Duval V., Aujol J. F., and Vese L., "A Projected Gradient Based Color Image Decomposition,"*Lecture Notes in Computer Science, springer*, Vol. 5567, pp. 295-306, 2009.
30. Iglesias J. E., Thompson P., and Tu Z., "A spatially variant mixture model for diffusion weighted MRI: Application to image denoising,"*Journal of Medical Physics*, Vol.38, pp. 4350-4364, 2011.
31. Loris I., Bertero M., Mol C. D., Zanella R., and Zanni L., "Accelerating gradient projection methods for ℓ_1-constrained signal recovery by steplength selection rules,"*Journal of Applied and Computational Harmonic Analysis, Elsevier*, Vol. 27, pp. 247-254, 2009.
32. Bertsekas D. P., "Projected Newton methods for optimization problems with simple constraints,"*SIAM Journal on Control and Optimization*,Vol. 20, pp. 221-246, 1982.
33. Gafni E. M., and Bertsekas D. P., "Convergence of a Gradient Projection Method,"*Massachusetts Institute of Technology, Laboratory for Information and Decision Systems*, pp. 1-12, 1982.
34. Beck A., and Teboulle M., "Gradient-Based Algorithms with Applications to Signal Recovery Problems,"*Convex Optimization in Signal Processing and Communications, Cambridge*, pp. 42-88, 2010.
35. Soman K. P., and Ramanathan R., "Digital Signal and Image processing-The Sparse way,"*Elsevier*, pp. 408-416, 2012.
36. Kranauskas J., "Accelerated Calculation of Gabor Features in Spatial Domain,"*Elektronika Ir Elektrotechnika*, Vol. 97, pp. 39, 2010.
37. Morrow M. G., Welch T. B., and Wright C. H. G., "A Host Port Interface Board to Enhance the TMS320C6713 DSK,"*IEEE Proceedings of Intl. Conference on Acoustics Speech and Signal Processing*, Vol. 2, pp. 969-972, 2006.
38. TMS320C6713 DSK, Technical Reference, DSP Development Systems, *Spectrum Digital Corporation*, 2003.
39. Kaymak E., Atherton M. A., Rotter K. R. G., and Millar B., "Real-Time Adaptive Filtering of Dental Drill Noise Using a Digital Signal Processor,"*In: 7th Intl. Workshop on Research and Education in Mechatronics, The Royal Institute of Technology, Stockholm*, 2006.
40. Zapata J., and Ruiz R., "Rapid Development of Real-Time Applications Using MATLAB/Simulink on TI C6000-based DSP,"*In Proceedings of the 5th WSEAS International Conference on Education and Educational Technology, Spain*, 2006, pp. 104-110.
41. Golabian S., Lucas C., Jamali M. R., and Afrasiabi M., "Implementation of the Emotional Controller Using DSK TMSC320 Digital Signal Processor,"*In: CSIT Proceedings*, pp. 477-480, 2009.
42. Abdullah M. F., Hashim N. M. Z., Saad N. M., Hadi N. A. A., Salleh A., and Jaafar A. S., "Sensors Application of Digital Signal Processing,"*International Journal for Advance Research in Engineering and Technology*, Vol. 3, pp.24-28, 2015.